

Terahertz electro-absorption effect enabling femtosecond all-optical switching in semiconductor quantum dots

M. C. Hoffmann,^{1,a)} B. S. Monozon,² D. Livshits,³ E. U. Rafailov,⁴ and D. Turchinovich^{5,b)}

¹Max Planck Research Department for Structural Dynamics, University of Hamburg, CFEL, 22607 Hamburg, Germany

²Department of Physics, State Marine Technical University, Lotsmanskaya 3, 190008 St. Petersburg, Russia

³Innolume GmbH, Konrad-Adenauer-Allee 11, 44263 Dortmund, Germany

⁴School of Engineering, Physics, and Mathematics, University of Dundee, Dundee DD1 4HN, United Kingdom

⁵DTU Fotonik - Department of Photonics Engineering, Technical University of Denmark, DK-2800 Kgs. Lyngby, Denmark

(Received 24 September 2010; accepted 25 October 2010; published online 8 December 2010)

We demonstrate an instantaneous all-optical manipulation of optical absorption in InGaAs/GaAs quantum dots (QDs) via an electro-absorption effect induced by the electric field of an incident free-space terahertz signal. A terahertz signal with the full bandwidth of 3 THz was directly encoded onto an optical signal probing the absorption in QDs, resulting in the encoded temporal features as fast as 460 fs. The instantaneous nature of this effect enables femtosecond all-optical switching at very high repetition rates, suggesting applications in terahertz-range wireless communication systems with data rates of at least 0.5 Tbit/s. © 2010 American Institute of Physics. [doi:10.1063/1.3515909]

Modern optical communication systems are reaching Tbit/s data rates in single serial communication channels.¹ Time and bandwidth considerations require that optical signals with femtosecond duration and terahertz (THz) bandwidth must be used as data symbols in such systems. In order to implement a wireless (sub)Tbit/s system, such as e.g., radio-over-fiber (RoF) system, the signal frequency must be in the THz range,² and femtosecond, single-cycle THz pulses should be used as data symbols. The means to encode such ultrafast THz signals onto an optical carrier at (sub)THz repetition rate should also be provided.

It was recently demonstrated that a continuous-wave (cw) THz signal originating from a cryogenically cooled quantum-cascade laser (QCL) can be encoded onto a cw optical carrier propagating through the waveguide comprising the QCL by THz-induced phase modulation via nonlinear-optical frequency mixing. As a result, the THz-spaced sidebands were observed in the spectrum of cw optical carrier.³

In this work we demonstrate femtosecond all-optical switching of optical absorption in InGaAs/GaAs quantum dots (QDs) via the *instantaneous* electro-absorption effect induced by the electric field of an incident THz pulse. As a result, we achieved a direct all-optical encoding of a free-space, ultrafast, high-bandwidth, and high repetition rate THz signal onto an optical signal probing the absorption in the QDs.

The electro-absorption effect in a QD, a quantum-confined Stark effect⁴ (QCSE), arises from the tilt in the confinement potential of a semiconductor nanostructure in the applied electric field E and manifests itself in two ways: (i) in a decrease of the optical transition energy between electron and hole states (Stark shift) and (ii) in a spatial separation of the envelope wavefunctions of electrons ψ_e and holes ψ_h in the presence of the electric field, which leads to a

smaller wavefunction overlap integral $M(E) = \langle \psi_e | \psi_h \rangle$. The value of $|M(E)|^2$ dictates the optical transition probability, and the optical absorption coefficient is directly proportional to it. Thus, the optical absorption can be manipulated by the applied electric field. In the case of a spatially symmetric confinement potential at $E=0$, the strength of the electro-absorption modulation effect only depends on the *absolute value* of the electric field and not on its sign.

Instead of applying the modulating electric field to the whole QD structure via the hard-wired electrodes, which would slow down the modulation rate due to a large RC-constant involved, we modulate the confinement potential of the QDs (which are the smallest possible semiconductor elements with a negligible RC constant) *directly* by the electric field of single-cycle THz pulses directed at the QD sample at normal incidence angle.

The sample used in our experiments was an InGaAs/GaAs QD-based semiconductor saturable absorber mirror (SESAM), comprising of a broadband GaAs/Al_{0.9}Ga_{0.1}As distributed Bragg reflector (DBR), and a QD absorber layer featuring 80 layers of submonolayer-grown In_{0.5}Ga_{0.5}As/GaAs QDs with the diameter of around 10 nm and the height of around 7 nm, alternated by the GaAs barriers of 10–14 nm thickness. Eight of these barriers were grown at low temperature (LT) in order to provide for the fast SESAM partial recovery with the exponential time constant of 4.3 ps for mode-locked laser applications, unrelated to this work. The QD absorber layer and the DBR were grown on a (450 ± 25) μm thick, <100>-oriented semi-insulating GaAs substrate. The small-signal optical reflectivity spectra of the whole QD sample, and of a bare DBR measured prior to the growth of the QD absorber layer, are shown in Fig. 1. The dip in the reflectivity of a QD sample positioned around 1040 nm is due to ground-state absorption in the QDs. The absence of in-plane conductivity due to the carriers occupying the QD ground state and a 35 ps long carrier thermalization time were observed in a similarly grown structure, dem-

^{a)}Electronic mail: matthias.c.hoffmann@desy.de.

^{b)}Electronic mail: dmtu@fotonik.dtu.dk.

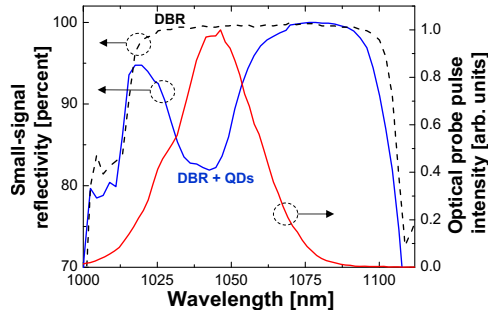


FIG. 1. (Color online) Small-signal reflectivity spectrum of the whole QD sample (solid line), a bare DBR (dashed line), and the intensity spectrum of the probe laser pulse at QD ground state resonance at 1040 nm.

onstrating the strong carrier confinement to the QDs at room temperature.⁵

Single-cycle THz pulses were generated by optical rectification of 800-nm, 80 fs long Ti:sapphire laser pulses of 2 mJ energy in a lithium niobate crystal at 1 kHz repetition rate using the tilted pulse-front technique,⁶ yielding THz pulse energies of 2 μ J. The THz pulses were characterized in the time-domain using a standard free-space electro-optic sampling in a combined “active-passive”⁷ 0.2 mm $\langle 110 \rangle$ – 2 mm $\langle 100 \rangle$ undoped GaP crystal, and showed a spectrum covering the range of 0.2–3 THz. The peak electric field of the strongest THz transient was estimated⁸ to be 220 kV/cm in air. The THz waveform and its amplitude spectrum are shown in Fig. 2(a). A weak optical probe pulse around the wavelength of 1040 nm, coinciding with the ground state absorption feature in the QDs (see Fig. 1), was produced by conversion of part of the 800 nm laser output, using an optical parametric amplifier.

We performed a THz pump - optical probe experiment on our sample, where the probe pulse reflectivity off the QD

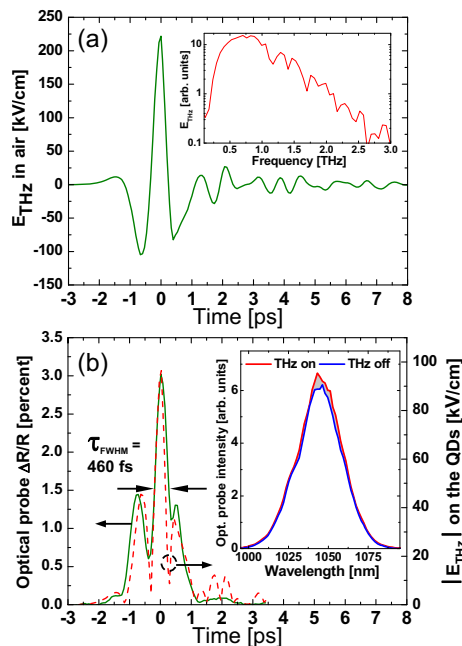


FIG. 2. (Color online) (a) Electric field in free-space as a function of time of the THz pulse with peak field strength of 220 kV/cm. Inset: its amplitude frequency spectrum. (b) Solid line: $\Delta R/R$ of the probe signal at 1040 nm in the QD sample, under influence of the incident THz pulse from (a). Dashed line: absolute value of the electric field in the THz pulse from (a) experienced by the QDs. Inset: intensity spectrum of the optical probe signal with and without peak electric field of the THz pulse from (a) on the QDs.

structure was modulated by the incident THz pulse. We measured the *absolute value* and the *sign* of the change in the optical probe reflectivity as a function of time-delay between the optical probe and THz pump pulses, using the photodiodes in a balanced detection arrangement. The angles of incidence on the sample (with respect to the normal) of the pump THz and probe optical beams were 0° and 10° , respectively. The optical probe signal interacted with the QDs twice: on the way to and from the DBR. However, the total thickness of the QD absorber layer, including GaAs barriers, and spacer and cladding layers, is only about 1.2 μ m, thus the interaction of both the THz pulse and the probe pulse with the QDs can be viewed as point interactions. All our measurements were performed at room temperature and in ambient atmospheric conditions. The dips in the amplitude spectrum of the THz signal in Fig. 2(a) are absorption lines of atmospheric water vapor.

In Fig. 2(b) our main result, a modulation of the reflectivity of the optical probe $\Delta R/R$, is shown, along with the absolute value of the electric field of the THz pulse $|E_{\text{THz}}|$, experienced by the QDs. The latter was calculated taking into account the THz field transmission coefficient at the sample GaAs interface of 0.435. The observed $\Delta R/R$ of the optical signal follows the shape of $|E_{\text{THz}}|$ in a temporally coherent manner, reproduces most of the features of the THz signal, and does not exhibit exponential-like decay features attributed to a relaxation process of any sort. The THz pulse features as fast as 460 fs at full width at half maximum are encoded all-optically onto the probe signal transmitted through the QDs. Obviously, these femtosecond-scale features cannot originate from a carrier depletion mechanism in QDs related to carrier trapping from the QDs onto lattice defects in the LT-GaAs barriers. This process with a decay time constant of 4.3 ps is nearly ten times slower than the observed fast modulations. The maximum observed $\Delta R/R$ value was about 3%, at the peak THz electric field on the QDs of 96.5 kV/cm. Following Ref. 9 we calculated the small-signal loss S experienced by the optical probe with the spectrum $I(\lambda)$ in the QDs as $S = \int_{\lambda} I(\lambda) [R_{\text{DBR}}(\lambda) - R_{\text{QD}}(\lambda)] d\lambda / \int_{\lambda} I(\lambda) d\lambda = 10.3\%$, where $R_{\text{DBR, QD}}$ are the reflectivity spectra of the bare DBR and of the whole QD sample (see Fig. 1). We were thus able to reach a 30% modulation of the QD absorption experienced by the optical probe. This is comparable to the modulation depth observed in resonantly probed quantum wells (QWs) at similar static bias field strengths.⁹ When the probe wavelength was de-tuned from the QD ground state resonance, the magnitude of $\Delta R/R$ signal decreased by an order of magnitude, proving that the observed modulation is indeed due to the interaction of the QDs with the THz field. None, or very weak dependency of the electro-absorption modulation strength on the polarizations of THz and optical signals, respectively, was observed, as is indeed expected from the three-dimensional QD geometry.

The sign of the observed reflectivity change $\Delta R/R$ is positive, corresponding to a *decrease* in optical absorption at the probe wavelength in the presence of THz electric field. This positive sign of $\Delta R/R$ suggests that both manifestations of the QCSE may play a role: overall absorption quenching; and Stark shift of the QD absorption spectrum toward longer wavelengths, i.e., out of the probe pulse spectrum.⁹ The inset of Fig. 2(b) shows the spectrum of the

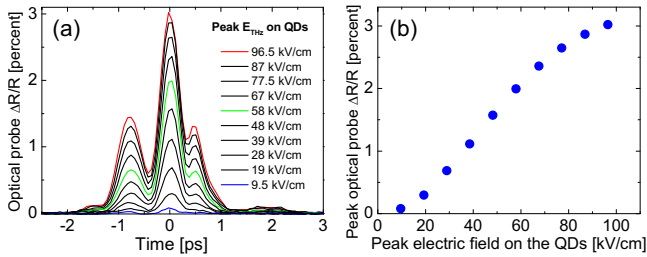


FIG. 3. (Color online) (a) $\Delta R/R$ of the optical probe signal in the QD sample, under influence of the incident THz pulses with variable peak field strength. (b) Peak values of $\Delta R/R$ of the signals from (a), as a function of peak THz field on the QDs.

optical probe pulse in the case when the maximum of the THz pulse was in temporal overlap with the probe pulse, and when the THz pulse was blocked. The change in the probe pulse amplitude is more or less spectrally homogeneous, suggesting that the absorption quenching in the QDs is likely to be a dominating electro-absorption modulation effect here.

Figure 3(a) shows the optical probe modulation signals $\Delta R/R$ for different THz field strengths. The THz electric field was controlled using a pair of wire-grid polarizers.¹⁰ In Fig. 3(b) the peak value of $\Delta R/R$ as a function of the peak THz electric field experienced by the QDs is shown, demonstrating a pronounced nonlinear scaling with the electric field, typical for the QCSE.⁴

We note that THz-induced electro-absorption modulation in semiconductors has been studied in the past theoretically.¹¹ Recently, it was observed at the exciton resonances in QWs¹² and carbon nanotubes.¹³ The excitons were polarized by the THz field in the plane of QWs or along the nanotube long dimension. Stronger THz fields lead to ionization of excitons in QWs.¹² The THz modulation rate limit of around 1 THz was observed in Ref. 13, and was related to the exciton dephasing time (also see discussion in Ref. 12). In the case of QDs, the modulation rate should probably be limited by the THz frequencies high enough to excite the intraband transitions in the QDs, i.e., by the frequencies of 10 THz and higher.

Finally, in Fig. 4 we show the modulation of optical absorption in the QDs induced by a *train of THz pulses* incident at high repetition rate. This THz pulse train originated from multiple reflections of a single THz pulse within the sample, which was attached to a metal mirror with the back

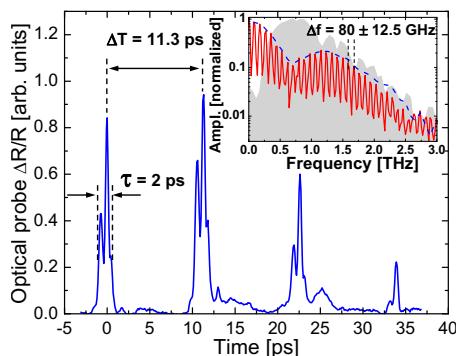


FIG. 4. (Color online) $\Delta R/R$ of the optical probe signal in the QDs, provided by the multiple reflections of a single THz pulse in the QD sample. Inset: amplitude Fourier spectra of the isolated first $\Delta R/R$ modulation pulse around 0 ps (dashed line), and of the full multipulse sequence. Background: amplitude spectrum of a single THz pulse.

side of its substrate. The individual pulses of $\Delta R/R$ have a temporal width of around 2 ps. Importantly, the contrast between the peak $\Delta R/R$ and the background is rather high. A certain reshaping of $\Delta R/R$ pulses in the sequence is due to the dispersion and scattering of the THz pulse experiencing multiple reflections within the sample. The interpulse interval of 11.3 ps (i.e., repetition rate of 88 GHz) corresponding to the round-trip time of the THz pulse within the sample, shows the possibility of 88 Gbit/s data rate using this electro-absorption modulation scheme. The ratio of interpulse interval to the individual pulse duration 11.3 ps/2 ps = 5.65 suggests that the demonstrated data rate can be scaled accordingly, and crosstalk-free data rates of 88 Gbit/s \times 5.65 = 0.5 Tbit/s can be achieved.

In the inset of Fig. 4, the amplitude Fourier spectra of the isolated $\Delta R/R$ pulse and of the whole multipulse sequence are shown, with the amplitude spectrum of the single THz pulse in the background. It can be clearly seen that the full bandwidth of the THz pulse of 3 THz is encoded onto the optical probe signal, and the repetition rate is also reflected in the spectrum. These Fourier spectra are analogous to the THz sidebands observed in work.³

In conclusion, we have demonstrated instantaneous and polarization-independent electro-absorption modulation in QDs on the order of several percent, by the broadband THz pulses incident from a free-space. This effect may find its applications in future (sub)Tbit/s RoF systems, as well as in general-purpose coherent THz-to-optical detectors/encoders. Optimization of interaction of QDs with THz field^{14,15} can lead to a THz electro-absorption modulator controlled by the low switching fields.

We are grateful to Max Planck Society and EU FP7 Programme (FAST-DOT, Grant No. 224338) for partial financial support, and to A. Cavalleri (University of Hamburg), A.-P. Jauho (DTU Nanotech), and K. Yvind and J. M. Hvam (DTU Fotonik) for valuable discussions.

¹H. C. H. Mulvad, M. Galili, L. K. Oxenløwe, H. Hu, A. T. Clausen, J. B. Jensen, C. Peucheret, and P. Jeppesen, *Opt. Express* **18**, 1438 (2010).

²J. Federici and L. Moeller, *J. Appl. Phys.* **107**, 111101 (2010).

³S. S. Dhillon, C. Sirtori, J. Alton, S. Barbieri, A. De Rossi, H. E. Beere, and D. A. Ritchie, *Nat. Photonics* **1**, 411 (2007).

⁴D. A. B. Miller, D. S. Chemla, T. C. Damen, A. C. Gossard, W. Wiegmann, T. H. Wood, and C. A. Burrus, *Phys. Rev. Lett.* **53**, 2173 (1984).

⁵H. P. Porte, P. U. Jepsen, N. Daghestani, E. U. Rafailov, and D. Turchinovich, *Appl. Phys. Lett.* **94**, 262104 (2009).

⁶K.-L. Yeh, M. C. Hoffmann, J. Hebling, and K. A. Nelson, *Appl. Phys. Lett.* **90**, 171121 (2007).

⁷D. Turchinovich and J. I. Dijkhuis, *Opt. Commun.* **270**, 96 (2007).

⁸F. Blanchard, L. Razzari, H. C. Bandulet, G. Sharma, R. Morandotti, J. C. Kieffer, T. Ozaki, M. Reid, H. F. Tiedje, H. K. Haugen, and F. A. Hegmann, *Opt. Express* **15**, 13212 (2007).

⁹X. Liu, E. U. Rafailov, D. Livshits, and D. Turchinovich, *Appl. Phys. Lett.* **97**, 051103 (2010).

¹⁰M. C. Hoffmann and D. Turchinovich, *Appl. Phys. Lett.* **96**, 151110 (2010).

¹¹K. Johnsen and A.-P. Jauho, *Phys. Rev. B* **57**, 8860 (1998).

¹²H. Hirori, M. Nagai, and K. Tanaka, *Phys. Rev. B* **81**, 081305(R) (2010).

¹³T. Ogawa, S. Watanabe, N. Minami, and R. Shimano, *Appl. Phys. Lett.* **97**, 041111 (2010).

¹⁴M. A. Seo, H. R. Park, S. M. Koo, D. J. Park, J. H. Kang, O. K. Suwal, S. S. Choi, P. C. M. Planken, G. S. Park, N. K. Park, Q. H. Park, and D. S. Kim, *Nat. Photonics* **3**, 152 (2009).

¹⁵D. Turchinovich, patent application PCT/DK2010/050200, 05 August (2009).